Collinear type II second-harmonic-generation frequency-resolved optical gating for the characterization of sub-10-fs optical pulses

L. Gallmann, G. Steinmeyer, D. H. Sutter, N. Matuschek, and U. Keller

Ultrafast Laser Physics Laboratory, Institute of Quantum Electronics, Swiss Federal Institute of Technology, ETH Hönggerberg–HPT, CH-8093 Zürich, Switzerland

Received May 27, 1999

For the first time to our knowledge, we demonstrate a collinear frequency-resolved optical gating (FROG) technique that is suitable for the characterization of sub-10-fs pulses. This FROG variant does not suffer from geometrical blurring effects, and a temporal resolution of 1 fs can be achieved without the need for additional aperturing. The apparatus is suitable for subnanojoule pulse energies. We apply this technique for the full characterization of pulses from a Kerr-lens mode-locked Ti:sapphire laser. © 2000 Optical Society of America

OCIS codes: 320.0320, 320.5550, 320.7100, 120.5050.

Pulses of two optical cycles or fewer have been generated by external pulse compression,[1,2] optical parametric amplification,[3] and more recently directly from laser oscillators.[4,5] The strongly modulated spectra observed in these experiments indicate a fairly complex pulse shape. For this situation, pure autocorrelation methods can provide only a rough estimate of pulse duration. Among the methods that allow for a more precise characterization, frequency-resolved optical gating[6] (FROG) has found the most widespread use. FROG has been demonstrated for pulses of 4.5-fs duration.[7] So far, in the sub-10-fs range, noncollinear setups have been used exclusively.

For few-cycle pulses, a limitation in a noncollinear beam geometry arises because of the finite crossing angle of the two beams. In this case the temporal delay between the two beams is different in the center and in the wings of the spatial beam profile. For this reason, collinear geometries have always been preferred for autocorrelators in the sub-10-fs range. To keep geometrical blurring artifacts small and to prevent temporal resolution from being reduced, one has to choose a crossing angle as small as possible.[8] For example, an overlap of the two beams at the $1/e$ points in the far field results in a temporal resolution of 0.15 optical cycle, i.e., 0.4 fs at an 800-nm center wavelength.[7] To avoid interference of the two beams without excessive geometrical blurring in noncollinear FROG, one chooses a larger crossing angle and images the central part of the conversion zone onto an aperture.[7] In principle, this procedure allows for nearly arbitrarily high temporal resolutions. For extremely large bandwidths, care has to be taken not to introduce spectral shaping at the aperture, for example, as a result of a possible frequency-dependent laser mode size.[5,9]

In this Letter we present a sub-10-fs collinear FROG apparatus based on type II phase matching. Recently, collinear type II second-harmonic generation (SHG) FROG was demonstrated for the measurement of 20-fs pulses in the focus of a high-numerical-aperture objective.[10] Here we discuss the modifications and conditions needed for ultrabroadband operation of a collinear type II SHG FROG apparatus.

In addition to fulfilling the usual bandwidth requirements, one must take particular care to avoid polarization-dependent pulse shaping in a type II setup. Otherwise, an asymmetry of the measured FROG traces will occur. To avoid polarization dependence of the beam splitting, we use near-normal 4° incidence rather than the 45° conventionally used (see Fig. 1). This scheme allows for a polarization-independent bandwidth of more than 400 nm. Asymmetry of the FROG trace can also be caused by group-velocity mismatch (GVM) in the nonlinear crystal. This axisymmetry can easily be avoided by use of a sufficiently thin nonlinear crystal, whose use is already dictated by the phase-matching bandwidth requirements.

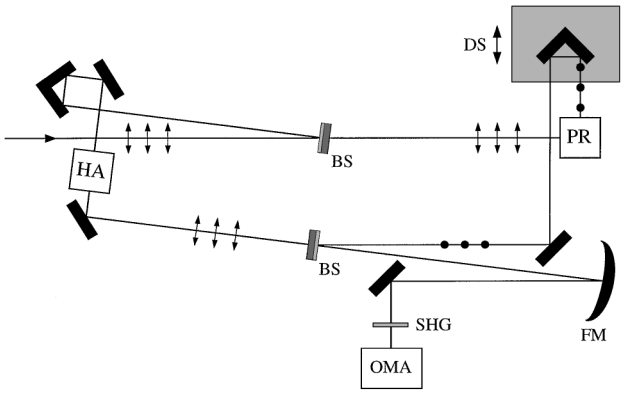

Fig. 1. Collinear type II SHG FROG setup: BS's, beam splitters; PR, periscope for polarization rotation; HA, periscope for height adjustment; FM, focusing mirror (25.6-cm radius of curvature); SHG, nonlinear crystal (10-μm-thick type II ADP); OMA, optical multichannel analyzer. Filled circles and arrows on the beam path display the polarization state of the beam. The black filled shapes represent silver-coated mirrors.

0146-9592/00/040269-03$15.00/0

With the crystal thickness approaching the coherence length, non-phase-matched SHG processes will make nonnegligible contributions to the observed signal. For a 10-μm β-barium borate crystal (point group $3m$) a significant contribution of second-harmonic radiation is generated by the square nonlinearity tensor element d_{31}.[11] This light is polarized along the extraordinary axis, as is the type II signal. This gives rise to interference. To avoid these delay-dependent distortions of the FROG trace, we chose a material with higher crystal symmetry. In our apparatus, we employ a 10-μm-thick ammonium dihydrogen phosphate (ADP) crystal (point group $\bar{4}2m$). Now only one undesired mixing process is contributing to the signal: The d_{25} tensor element generates SHG radiation polarized along the ordinary axis. Because this light is polarized orthogonally to the FROG signal, it is easily rejected by a polarizer or subtracted as a constant background.

The ultimate limitation of temporal resolution in a type II SHG FROG arises from GVM in the nonlinear crystal. In principle, a GVM between the two orthogonally polarized fundamental pulses causes an effect similar to the geometrical blurring effect in a type I SHG FROG. In a 10-μm ADP crystal, GVM limits the temporal resolution to 1.2 fs. This is either smaller than or of the order of values published for type I SHG FROG.[7,8,12]

Figure 1 depicts our collinear type II SHG FROG setup. Note the use of all-reflective optics wherever possible and the dispersion-balanced configuration of the beam-splitting scheme. Two identical dielectric beam splitters (CVI Laser Corporation) with 300-μm thickness are used. The beam is polarized better than 1:100 after the out-of-plane polarization rotation. Unwanted type I radiation is suppressed by a broadband Glan–Thompson polarizer. Additional filtering is required for suppression of fundamental light. For this purpose, we use 1 mm of Schott BG3 colored glass and four bounces on two broadband dielectric UV–visible mirrors (New Focus). The spectra are recorded on a 0.3-m optical multichannel analyzer equipped with a 300-groove/mm grating and a UV-enhanced 1024 $\times$ 128 pixel CCD camera. Wavelength-dependent sensitivity of the detection system is measured with a calibrated white-light source. The recorded FROG traces are corrected for spectral dependence of conversion and detection efficiency.

To demonstrate the ultrafast type II FROG setup, we characterize pulses from our Kerr-lens mode-locked Ti:sapphire laser.[5] These pulses have a Fourier limit of 7.4 fs. Measured and reconstructed FROG traces with a grid size of 128 $\times$ 128 points are shown in Fig. 2. The measured FROG trace does not exhibit any indications of excess GVM or polarization-dependent pulse shaping, as is indicated by the symmetry of the measurement. Excellent symmetry is observed even for the broadest spectra with Fourier limits as short as 5.3 fs. Pulse reconstruction is performed with commercial software (Femtosoft Technologies). The FROG error of this reconstruction amounts to 0.0032. Some imperfections in the measured FROG trace can be attributed to the residual interference fringes in the unfiltered input data. Noise increases in the spectral wings as a result of the reduced colored glass filter transmission at these wavelengths. In Fig. 3 the reconstructed pulse profile and spectrum are shown. The width of the temporal intensity profile is 9 fs, indicating uncompensated chirp. The divergence of the spectral phase below 700 nm and above 900 nm is caused by the phase properties of the output coupler. In the time domain, together with the modulated shape of the spectrum, this uncompensated high-order dispersion results in a pulse pedestal with less than 15% of the pulse peak power. The small sinusoidal oscillations observed in the spectral phase are explained by group-delay oscillations of the double-chirped mirrors[13] used for external dispersion compensation.

To supplement the internal consistency checks of the FROG method (Fig. 4),[6] we made comparisons with independent pulse-characterization tools. Figure 3 shows a comparison of the reconstructed and the measured fundamental pulse spectra. Some of the slight disagreement between the two spectra or between the measured and the calculated frequency marginal (Fig. 4) can be attributed to frequency-dependent mode-size effects. These effects are a well-known problem that is inherent in Kerr-lens mode-locked lasers.[9]

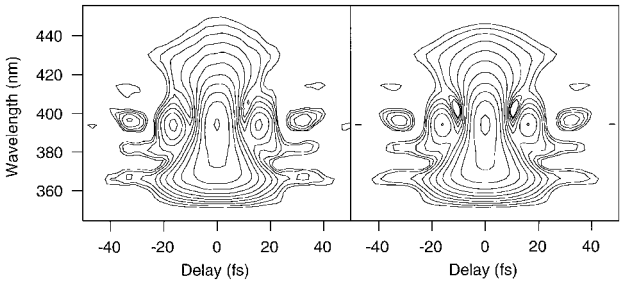

Fig. 2. Measured and reconstructed FROG trace (logarithmic contour spacing, lowest contour at 0.6% of peak). For display purposes, residual fringes in the measured FROG trace have been removed by Fourier filtering. They are not strong enough to affect the reconstruction of the pulse.

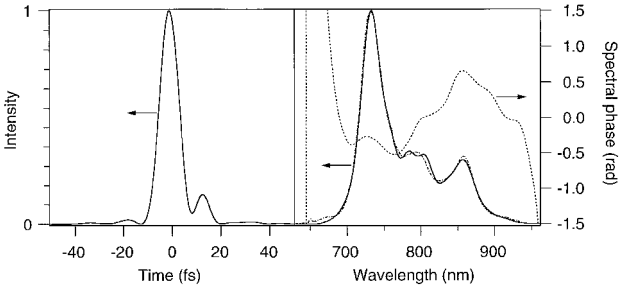

Fig. 3. Reconstructed temporal intensity profile with a full width at half-maximum of 9 fs (left), spectrum (right, solid curve), and spectral phase (right, dashed curve). Additionally, the independently measured spectrum is plotted at the right (dashed-dotted curve). Intensity and phase are scaled on the left and right vertical axes, respectively.

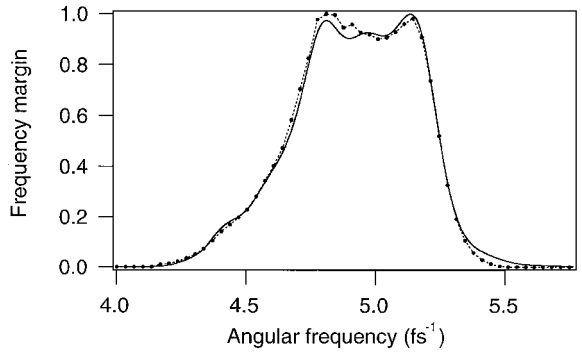

Fig. 4. Measured frequency marginal (filled circles, dashed curve) and autoconvolution of the separately recorded fundamental spectrum (solid curve).

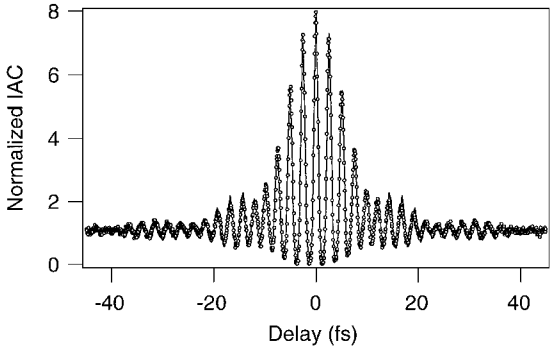

Fig. 5. Comparison of the independently measured IAC (circles) with the IAC calculated from the reconstructed spectrum and phase (solid curve).

Figure 5 depicts the good agreement of the interferometric autocorrelation (IAC) calculated from the FROG data with the measured IAC. We observed that the assumption of analytical pulse shapes usually leads to unsatisfying fits of the IAC and often to large errors in the estimated pulse duration. For example, a sech^2 fit to the IAC would yield a pulse duration of 7 fs, a duration significantly below the 9 fs measured with FROG and below the transform limit of the spectrum. Clearly, if the spectrum already indicates strong deviations from simple analytical shapes, deconvolution of the autocorrelation under an *a priori* assumption of such a particular pulse shape is not justified. This finding strongly confirms the need for accurate and easy-to-use characterization tools for sub-10-fs pulses.

Complete characterization of pulses in the sub-10-fs regime is still a challenging task. At first sight, the type II SHG-FROG geometry seems to introduce additional complications. However, suppression of polarization-dependent pulse shaping and GVM can easily be accomplished by proper optical design. In turn, geometrical blurring effects are completely avoided in a collinear technique. The temporal resolution can be calculated exclusively from nonlinear crystal properties. Moreover, the apparatus is simple to align. Sub-fs resolution of a type II SHG FROG can be achieved by use of low-dispersion nonlinear optical materials, such as KDP and ADP, with small GVM.

We gratefully acknowledge helpful discussions with R. Trebino and K. W. DeLong. This study was supported by the Swiss National Science Foundation. L. Gallmann's e-mail address is gallmann@iqe.phys.ethz.ch.

References

1. M. Nisoli, S. De Silvestri, O. Svelto, R. Szipöcs, K. Ferenz, C. Spielmann, S. Sartania, and F. Krausz, Opt. Lett. **22,** 522 (1997).
2. A. Baltuska, Z. Wei, M. S. Pshenichnikov, D. A. Wiersma, and R. Szipöcs, Appl. Phys. B **65,** 175 (1997).
3. A. Shirakawa, I. Sakane, M. Takasaka, and T. Kobayashi, Appl. Phys. Lett. **74,** 2268 (1999).
4. U. Morgner, F. X. Kärtner, S. H. Cho, Y. Chen, H. A. Haus, J. G. Fujimoto, E. P. Ippen, V. Scheuer, G. Angelow, and T. Tschudi, Opt. Lett. **24,** 411, 920 (1999).
5. D. H. Sutter, G. Steinmeyer, L. Gallmann, N. Matuschek, F. Morier-Genoud, U. Keller, V. Scheuer, G. Angelow, and T. Tschudi, Opt. Lett. **24,** 631 (1999).
6. R. Trebino, K. W. DeLong, D. N. Fittinghoff, J. Sweetser, M. A. Krumbügel, and B. Richman, Rev. Sci. Instrum. **68,** 1 (1997).
7. A. Baltuska, M. S. Pshenichnikov, and D. A. Wiersma, IEEE J. Quantum Electron. **35,** 459 (1999).
8. G. Taft, A. Rundquist, M. M. Murnane, I. P. Christov, H. C. Kapteyn, K. W. DeLong, D. N. Fittinghoff, M. A. Krumbügel, J. N. Sweetser, and R. Trebino, IEEE Sel. Top. Quantum Electron. **2,** 575 (1996).
9. S. T. Cundiff, W. H. Knox, E. P. Ippen, and H. A. Haus, Opt. Lett. **21,** 622 (1996).
10. D. N. Fittinghoff, A. C. Millard, J. A. Squier, and M. Müller, IEEE J. Quantum Electron. **35,** 479 (1999).
11. V. G. Dmitriev, G. G. Gurzadyan, and D. N. Nikogosyan, in *Handbook of Nonlinear Optical Crystals*, A. E. Siegman, ed. (Springer-Verlag, Berlin, 1997), p. 24.
12. Z. Cheng, A. Fürbach, S. Sartania, M. Lenzner, C. Spielmann, and F. Krausz, Opt. Lett. **24,** 247 (1999).
13. N. Matuschek, F. X. Kärtner, and U. Keller, IEEE J. Quantum Electron. **35,** 129 (1999).